

# Selinene Volatiles Are Essential Precursors for Maize Defense Promoting Fungal Pathogen Resistance<sup>1</sup>[OPEN]

Yezhang Ding,<sup>a</sup> Alisa Huffaker,<sup>a</sup> Tobias G. Köllner,<sup>b</sup> Philipp Weckwerth,<sup>a</sup> Christelle A. M. Robert,<sup>c</sup> Joseph L. Spencer,<sup>d</sup> Alexander E. Lipka,<sup>e</sup> and Eric A. Schmelz<sup>a,2</sup>

<sup>a</sup>Section of Cell and Developmental Biology, University of California San Diego, La Jolla, California 92093-0380

<sup>b</sup>Department of Biochemistry, Max Planck Institute for Chemical Ecology, D-07745 Jena, Germany

<sup>c</sup>Institute of Plant Sciences, University of Bern, Bern CH-3013 Switzerland

<sup>d</sup>Illinois Natural History Survey, University of Illinois, Champaign, Illinois 61820

<sup>e</sup>Department of Crop Sciences, University of Illinois, Urbana, Illinois 61801

ORCID IDs: 0000-0001-5903-1870 (Y.D.); 0000-0002-3886-8433 (A.H.); 0000-0002-7037-904X (T.G.K.); 0000-0003-4757-563X (J.L.S.); 0000-0002-2837-734X (E.A.S.).

To ensure food security, maize (*Zea mays*) is a model crop for understanding useful traits underlying stress resistance. In contrast to foliar biochemicals, root defenses limiting the spread of disease remain poorly described. To better understand belowground defenses in the field, we performed root metabolomic profiling and uncovered unexpectedly high levels of the sesquiterpene volatile  $\beta$ -selinene and the corresponding nonvolatile antibiotic derivative  $\beta$ -costic acid. The application of metabolite-based quantitative trait locus mapping using biparental populations, genome-wide association studies, and near-isogenic lines enabled the identification of terpene synthase21 (*ZmTps21*) on chromosome 9 as a  $\beta$ -costic acid pathway candidate gene. Numerous closely examined  $\beta$ -costic acid-deficient inbred lines were found to harbor *Zmtps21* pseudogenes lacking conserved motifs required for farnesyl diphosphate cyclase activity. For biochemical validation, a full-length *ZmTps21* was cloned, heterologously expressed in *Escherichia coli*, and demonstrated to cyclize farnesyl diphosphate, yielding  $\beta$ -selinene as the dominant product. Consistent with microbial defense pathways, *ZmTps21* transcripts strongly accumulate following fungal elicitation. Challenged field roots containing functional *ZmTps21* alleles displayed  $\beta$ -costic acid levels over 100  $\mu\text{g g}^{-1}$  fresh weight, greatly exceeding in vitro concentrations required to inhibit the growth of five different fungal pathogens and rootworm larvae (*Diabrotica balteata*). In vivo disease resistance assays, using *ZmTps21* and *Zmtps21* near-isogenic lines, further support the endogenous antifungal role of selinene-derived metabolites. Involved in the biosynthesis of nonvolatile antibiotics, *ZmTps21* exists as a useful gene for germplasm improvement programs targeting optimized biotic stress resistance.

Plants are protected from a broad range of harmful biotic agents by initial perception events, signal transduction cascades, and the elicitation of defense metabolism (VanEtten et al., 1994; Harborne, 1999; Dangel et al., 2013; Huffaker et al., 2013). In maize (*Zea mays*), seedlings are largely protected from attack by a complex suite of hydroxamic acid-based defenses, termed benzoxazinoids, responsible for resistance to diverse threats spanning fungal pathogens and herbivores, including northern corn leaf blight (*Setosphaeria turcica*) and the European corn borer (*Ostrinia nubilalis*; Beck et al., 1957; Couture et al., 1971; McMullen et al., 2009a). Sixty years of research has resulted in a nearly complete metabolic and genetic benzoxazinoid pathway in maize involving over a dozen individual enzymes and metabolites (Frey et al., 2009; Meihls et al., 2013; Handrick et al., 2016). Additionally, diverse terpenoids and underlying terpene synthases (Tps) also have been demonstrated to play important protective roles (Degenhardt, 2009; Schmelz et al., 2014). As indirect defenses, herbivore-elicited terpene volatiles can function as diffusible signals to attract natural enemies, such as parasitoids and entomopathogenic nematodes, to

aboveground and belowground insect pests, respectively (Rasmann et al., 2005; Schnee et al., 2006).

Of the many biosynthetic classes of natural products, terpenoids are the most structurally diverse, with well over 25,000 established compounds. In addition to roles as phytohormone signals, specialized terpenoids mediate interorganism interactions and serve as chemical barriers (Gershenzon and Dudareva, 2007). In maize, terpene olefins are nearly ubiquitous components of induced aboveground and belowground volatile emissions acting as indirect plant defenses following biotic stress (Turlings et al., 1990; Degenhardt, 2009; Degenhardt et al., 2009a; Köllner et al., 2013). Maize terpene olefins also can serve as precursors for the localized production of nonvolatile antibiotic terpenoid defenses (Schmelz et al., 2014). While often undetectable at the level of volatile pathway intermediates, the inducible accumulation of nonvolatile terpenoid end products can limit the damage caused by fungi, herbivores, and oxidative stresses (Harborne, 1999; Ahuja et al., 2012). Despite significant advances, continuing discoveries in maize reveal that our collective knowledge of biochemical defenses and pathway

genes responsible for mitigating crop stress remains incomplete.

Decades of intensive research in related poaceous crops, such as rice (*Oryza sativa*), has revealed multiple pathways of inducible labdane-related diterpenoids, including momilactones, oryzalexins, and phyto-cassanes, that underlay protective responses to biotic and abiotic stress (Schmelz et al., 2014). More recently, complex arrays of acidic terpenoids have been detected in maize and include sesquiterpenoids derived from  $\beta$ -macrocarpene and diterpenoids derived from *ent*-kauranes, termed zealexins and kauralexins, respectively (Huffaker et al., 2011; Schmelz et al., 2014). From a biosynthetic pathway perspective, maize genes underlying the production of antifungal agents remain largely unknown. In the case of maize diterpenoid defenses, a specific *ent*-copalyl diphosphate synthase (Anther ear2; ZmAn2) is the only enzyme demonstrated in planta essential for kauralexin biosynthesis (Vaughan et al., 2015).

To uncover further defense pathways, we employed targeted metabolomic profiling on field-grown maize roots naturally exposed to combinations of herbivores and pathogens (Baldwin, 2012). Curiously, high levels of rarely encountered eudesmane sesquiterpenoids, including  $\beta$ -selinene and  $\beta$ -costic acid, dominated the chemical profiles of many samples. While not previously associated with maize,  $\beta$ -costic acid is known from the Asteraceae family, including false yellowhead (*Dittrichia viscosa*) and costus (*Saussurea costus*), and has been utilized in extracts for potent antibiotic activities against diverse organisms (Rao and Alvarez, 1981; Wu et al., 2006; Katerinopoulos et al., 2011). Despite the diverse phylogenetic occurrence in nature, a specific

pathway predominantly leading to  $\beta$ -costic acid has not been described in plants. To explore the maize  $\beta$ -costic acid pathway, combined genetic mapping approaches with the intermated B73  $\times$  Mo17 (IBM) population of recombinant inbred lines (RILs; Lee et al., 2002), the Goodman diversity panel (Flint-Garcia et al., 2005), and IBM near-isogenic lines (NILs; Eichten et al., 2011) were used for metabolite-based quantitative trait locus (mQTL) mapping. Biochemical characterization of the mQTL-identified Tps candidate utilized heterologous expression in *Escherichia coli* to confirm the identification of a comparatively product-specific  $\beta$ -selinene synthase. Transcript expression and metabolite analyses following elicitation with multiple pathogens and western corn rootworm (WCR; *Diabrotica virgifera virgifera*) larvae (Gray et al., 2009; Meinke et al., 2009; Miller et al., 2009; Spencer et al., 2009; Tinsley et al., 2013) were used to assess pathway activation. Concentrations of  $\beta$ -costic acid below those detected in field tissues were then used to examine in vitro antibiotic activity against five fungal species. Similarly, NILs were used to investigate in vivo root resistance following challenge with *Fusarium verticillioides* and *Fusarium graminearum*. Collectively, our results support the existence of a previously unrecognized  $\beta$ -costic acid pathway in maize that contributes to fungal pathogen resistance.

## RESULTS

### Identification of $\alpha$ - and $\beta$ -Selinene-Derived Products as Inducible Maize Sesquiterpenoids That Can Influence Generalist Root Herbivores

Our previous investigation of maize responses following stem herbivory and fungal elicitation enabled the discovery of two distinct biosynthetic classes of inducible acidic terpenoids (Huffaker et al., 2011; Schmelz et al., 2011). Similarly, experiments examining maize root defenses elicited by banded cucumber beetle (*Diabrotica balteata*) larvae and *F. verticillioides* infection confirmed shared responses in diverse tissue types (Vaughan et al., 2015). Given that predominant defenses change over ontogeny and that controlled laboratory experiments do not capture the full suite of biotic stresses in nature (Köllner et al., 2004a; Baldwin, 2012), we sought to expand our targeted metabolomic analyses to roots in the context of natural biotic challenge (Schmelz et al., 2004). As expected, mature visibly necrotic roots of field-challenged maize lines including hybrid sweet corn (variety Golden Queen) and the inbred Mo17 contained zealexins (Fig. 1A); however, chemically extracted samples unexpectedly also contained  $\alpha$ -selinene,  $\beta$ -selinene,  $\beta$ -costol,  $\alpha$ -costic acid, and  $\beta$ -costic acid (Fig. 1; Supplemental Fig. S1). In volatile collections of live Mo17 root emissions,  $\alpha$ -selinene,  $\beta$ -selinene (Fig. 2), and the aldehyde  $\beta$ -costal (Supplemental Fig. S1) were likewise detectable. As the major analyte, live field-collected Mo17 roots

<sup>1</sup> E.A.S. and A.H. gratefully acknowledge support by startup funds through the University of California San Diego, the DOE Joint Genome Institute Community Science Program (grant no. WIP 2568), and partial support for this work through a NSF-IOS Competitive Award (grant no. 1139329). With the support of Y. Yoshikuni, this research, or a portion thereof, was performed under the JGI-EMSL Collaborative Science Initiative and used resources at the DOE Joint Genome Institute and the Environmental Molecular Sciences Laboratory, which are DOE Office of Science user facilities. Both facilities are sponsored by the Office of Biological and Environmental Research and operated under contract numbers DE-AC02-05CH11231 (JGI) and DE-AC05-76RL01830 (EMSL).

<sup>2</sup> Address correspondence to eschmelz@ucsd.edu.

The author responsible for distribution of materials integral to the findings presented in this article in accordance with the policy described in the Instructions for Authors ([www.plantphysiol.org](http://www.plantphysiol.org)) is: Eric A. Schmelz (eschmelz@ucsd.edu).

E.A.S., A.H., and Y.D. conceived the original screening and research plans; Y.D. performed most of the experiments; P.W. provided technical assistance to Y.D.; Y.D., T.G.K., C.A.M.R., J.L.S., and A.E.L. designed the experiments and analyzed the data; E.A.S., Y.D., and A.H. conceived the project and wrote the article with contributions of all the authors; T.G.K., C.A.M.R., and A.E.L. supervised and completed the writing of specific sections.

[OPEN] Articles can be viewed without a subscription.

[www.plantphysiol.org/cgi/doi/10.1104/pp.17.00879](http://www.plantphysiol.org/cgi/doi/10.1104/pp.17.00879)

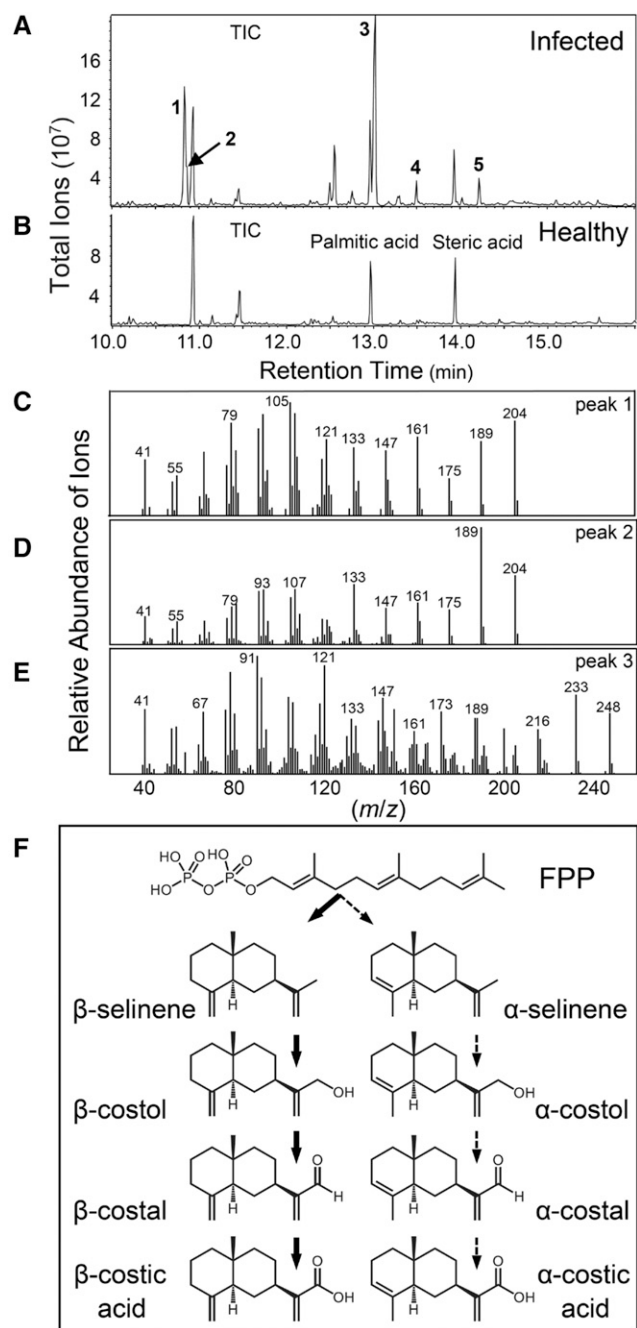


**Figure 1.**  $\beta$ -Selinene and  $\beta$ -costic acid can occur as major components of maize roots in field-grown plants. A and B, Visibly infected (A) and healthy (B) field-collected sweet corn (variety Golden Queen) root samples following trimethylsilyldiazomethane derivatization of carboxylic acids to corresponding methyl esters. Labeled peaks in representative gas chromatography (GC)/electron impact (EI)-mass spectrometry (MS) total ion chromatograms (TIC) are as follows: 1,  $\beta$ -selinene; 2,  $\alpha$ -selinene (shoulder); 3,  $\beta$ -costic acid; 4, zealexin A1; and 5, zealexin B1. The presence of common fatty acids, namely palmitic acid and steric acid, is unchanged in healthy root tissues and directly labeled for reference. C to E, Corresponding EI spectra (mass-to-charge ratio [ $m/z$ ]) of  $\beta$ -selinene (C),  $\alpha$ -selinene (D), and  $\beta$ -costic acid methyl ester (E) from maize field-collected roots. F, Proposed  $\alpha/\beta$ -costic acid biosynthetic pathway in maize starting from farnesyl diphosphate (FPP).

displaying visible necrosis emit predominantly  $\beta$ -selinene (Fig. 2). In contrast,  $\beta$ -selinene emission is absent in B73 roots; however, production reappears in select B73  $\times$  Mo17 RILs, such as IBM0287 (Fig. 2). Similar volatile emission results are observed in live Mo17 stems following inoculation with the necrotrophic fungal pathogen *Cochliobolus heterostrophus*, commonly known as southern leaf blight (Fig. 2). Consistent with root metabolite patterns, the reference genome inbred B73 (Schnable, 2009) remains void of  $\alpha$ - and  $\beta$ -selinene stem volatiles under identical conditions (Fig. 2). Qualitative metabolite differences between B73, Mo17, and select RILs provide empirical evidence for genetic variation in selinene biosynthesis and encourage the use of genetic mapping resources (Lee et al., 2002).

Our quantification of unexpectedly high levels of  $\beta$ -selinene and  $\beta$ -costic acid in field-collected maize roots was paired with casual field observations of adult *D. balteata* beetles on leaves. Given the broad host range of *D. balteata* larvae (Saba, 1970) and pest pressures exerted by WCR larvae, including the promotion of secondary disease (Flint-Garcia et al., 2009; Gray et al., 2009), we conducted controlled *Diabrotica*-maize interaction experiments. In growth chamber assays, tissue extracts of roots revealed both  $\beta$ -selinene and  $\beta$ -costic acid following damage by WCR larvae (Fig. 2). Given the high levels of selinene-derived metabolites observed in field-collected roots, additional assessments of WCR and *D. balteata* preference and performance were conducted on larvae. For both *Diabrotica* spp., we observed no influence of exogenously applied  $\beta$ -costic acid on root preference but found a significant inhibitory role of  $\beta$ -costic acid on *D. balteata* performance (Fig. 2).

#### Combined Linkage and Association Mapping Identifies the Maize Terpene Synthase *ZmTps21* as a Candidate Biosynthetic Gene

$\beta$ -Selinene was detected previously in the volatile profiles of pathogen-challenged maize tissue; however, the biosynthetic source and physiological function(s) have not been elucidated (Becker et al., 2014). Given our observation that selinene-derived pathway products can predominate in maize under specific conditions, we sought to identify the gene(s) responsible. We first employed the IBM RILs for mQTL mapping. As a predictable nonvolatile pathway end product,  $\beta$ -costic acid levels were analyzed in naturally challenged roots of 216 IBM RILs (Supplemental Table S1). Composite interval mapping (CIM) placed the locus in bin 9.05 (Fig. 3; Gardiner et al., 1993). For comparative purposes, the IBM RIL data also were explored using 173,984 single-nucleotide polymorphisms (SNPs) and association mapping via a general linear model (GLM; Bradbury et al., 2007) and a unified mixed linear model (MLM; Yu et al., 2006). All approaches supported a single statistically significant locus on chromosome 9 (Fig. 3; Supplemental Fig. S2). Additionally, we performed an elicited metabolite-based genome-wide association

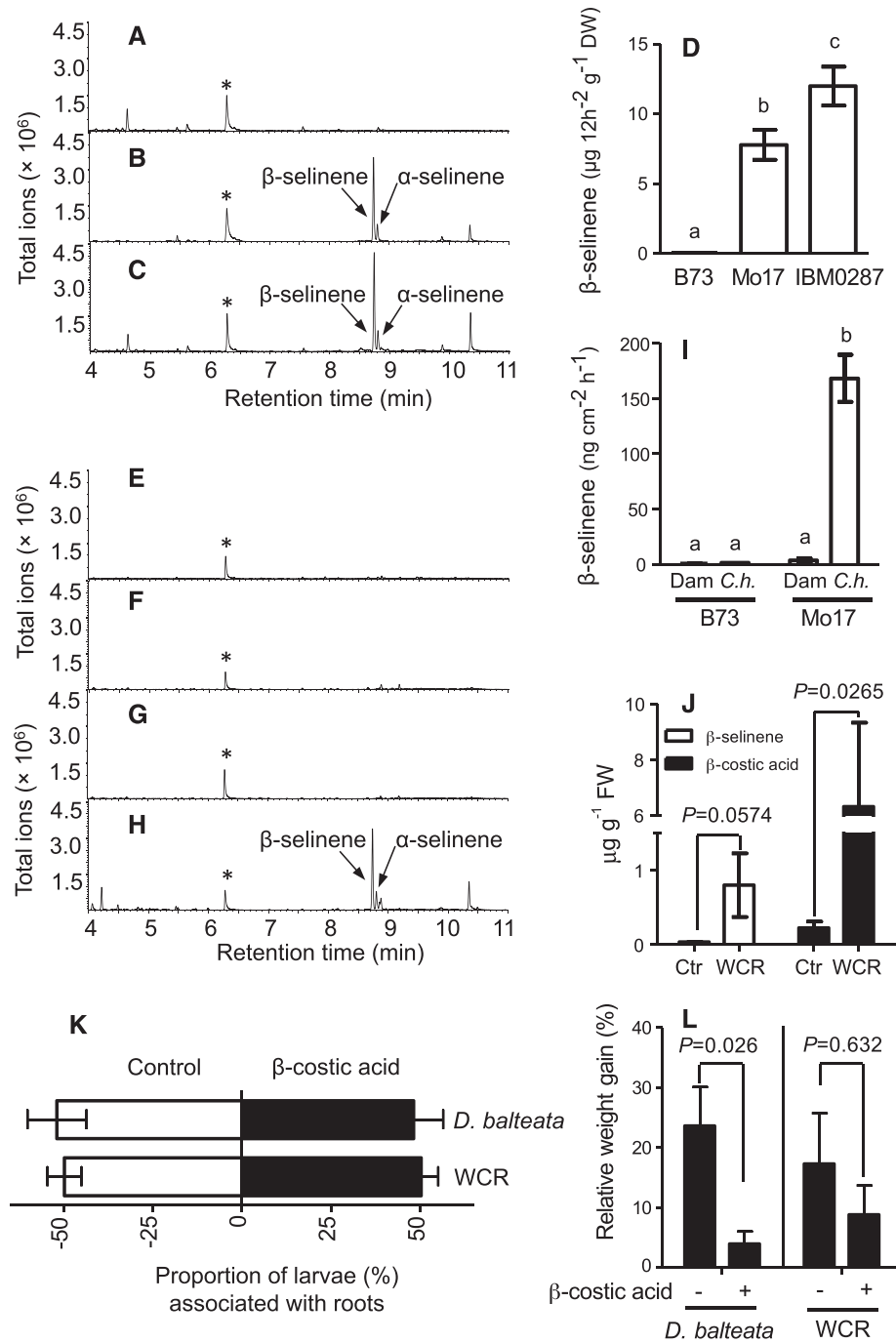


**Figure 2.**  $\beta$ -Selinene can exist as a dominant elicited volatile, and the pathway product  $\beta$ -costic acid can reduce herbivore performance. A to C, Representative GC coupled with flame ionization detection (FID) traces of volatile emissions collected from live roots of field-grown maize lines B73 (A), Mo17 (B), and IBM-RIL-0287 (C) 20 d after pollination. D, Average ( $n = 4$ ;  $\pm$ SE) quantity ( $\mu\text{g } 12 \text{ h}^{-2} \text{ g}^{-1}$  dry weight [DW]) of  $\beta$ -selinene volatiles emitted from respective maize roots. E to H, Representative GC-FID traces of emitted volatiles collected from living control B73 (E), *C. heterostrophus*-infected B73 (F), control Mo17 (G), and Mo17 *C. heterostrophus*-infected (H) stems. I, Average ( $n = 4$ ;  $\pm$ SE) quantity ( $\text{ng cm}^{-2} \text{ h}^{-1}$ ) of  $\beta$ -selinene emitted as a volatile from the stems of 5-week-old plants following damage and treatment with water (Dam) or with  $100 \mu\text{L}$  of  $1 \times 10^7$  spores *C. heterostrophus* (C.h.). Within plots D and I, different letters (a–c) represent significant differences (all ANOVAs,  $P < 0.05$ ; Tukey’s test corrections for multiple comparisons,  $P < 0.05$ ). J, Average ( $n = 4$ ;  $\pm$ SE) root tissue concentrations ( $\mu\text{g g}^{-1}$  fresh weight [FW]) of  $\beta$ -selinene and  $\beta$ -costic acid levels in the roots of IBM-RIL-0287 following 17 d of either no treatment (Ctr) or herbivory by WCR larvae (Student’s *t* test, one-tailed distribution, equal variance). K, Average WCR ( $n = 18$ ;  $\pm$ SE) and *D. balteata* ( $n = 57$ ;  $\pm$ SE) preference over 4 h for excised maize roots treated with either ethanol:water (15:85) alone (Control) or the same solution containing  $\beta$ -costic acid to achieve a root tissue concentration of  $100 \mu\text{g g}^{-1}$  fresh weight. Each replicate ( $n$ ) consisted of assays

study (mGWAS) using  $\beta$ -costic acid levels in greenhouse-grown inbreds from the Goodman diversity panel (Flint-Garcia et al., 2005). Similarly, we detected a single statistically significant locus on chromosome 9 (Fig. 3). An independent mGWAS replication conducted with field-grown plants yielded an identical result (Supplemental Fig. S2). The correspondence of physical QTL coordinates identified with IBM RILs and the replicated GWAS results (Fig. 3; Supplemental Fig. S2) robustly supported a single narrow locus controlling maize  $\beta$ -costic acid levels.

For additional confirmation, select B73  $\times$  Mo17 NILs were analyzed following stem elicitation (Eichten et al., 2011). B73 chromosomal segments introgressed into Mo17 dominating lines (specifically m012, m048, m050, and m062) were each deficient in the production of  $\beta$ -costic acid (Fig. 3). In contrast,  $\beta$ -costic acid production in NILs with introgressions of the Mo17 allele into the B73 genetic background (lines b047, b055, b069, and b157) was similar to that of Mo17 (Fig. 3; Supplemental Fig. S3), confirming the existence of the  $\beta$ -costic acid-associated locus in bin 9.05. Further analyses of additional NILs (b022, b033, m002, m065, and m092) narrowed the locus to 13 predicted genes isolated on bacterial artificial chromosome clones, AC213878 and AC204415 (Fig. 3). Of the remaining candidates, only a single uncharacterized gene (GRMZM2G011151) displayed significant sequence homology with known terpene synthases. Supportively, detailed examination of three independent association mapping results likewise demonstrated the presence of highly significant SNPs associated with the Tps candidate (GRMZM2G011151), termed *ZmTps21* (Supplemental Fig. S2). Genomic structure analysis of B73 *Zmtps21* revealed three predicted exons encoding a 297-amino acid protein lacking the conserved Tps catalytic domains, namely the DDXXD and RXR motifs (Fig. 3), which are essential for function (Chen et al., 2011). Collectively, these findings made B73 *Zmtps21* a parsimonious inactive  $\beta$ -selinene synthase pseudogene candidate meriting further examination.

In an attempt to isolate the Mo17 *ZmTps21* cDNA sequence, early reverse transcription-PCR trials with primers based upon B73 *Zmtps21* cDNA failed due to nucleotide polymorphisms. Eventually, a segment near the Mo17 *ZmTps21* 5' end of genomic DNA was obtained by PCR and sequenced. Alignments revealed that the segment near the Mo17 *ZmTps21* 5' end DNA fragment shared high sequence similarity with that of B73 *Zmtps21*. Therefore, the 5' end cDNA sequence of Mo17 *ZmTps21* was obtained by reverse transcription-PCR and extended by PCR with RACE using a cDNA

library to obtain the full-length Mo17 *ZmTps21* cDNA (Fig. 3; Supplemental Fig. S4). The deduced amino acid sequence of the open reading frame contained the conserved terpene synthase domains including the DDXXD (residues 325–329) and RXR (residues 288–290) motifs (Supplemental Fig. S4). The amino acid sequence of *ZmTps21* resembles (less than 60% identity) those of other plant sesquiterpene synthases and shares less than 40% sequence identity with previously characterized maize sesquiterpene synthases, such as *ZmTps6*, *ZmTps10*, *ZmTps11*, and *ZmTps23* (Supplemental Fig. S4). With only 30% identity at the amino acid level, Mo17 *ZmTps21* is even more distantly related to the *Ocimum basilicum* sesquiterpene synthase, which produces detectable levels of  $\beta$ -selinene as part of a complex blend (Supplemental Fig. S4; Iijima et al., 2004).

To understand the extent of genetic variation in *ZmTps21* alleles, we examined 15 commonly investigated inbreds. *ZmTps21* genomic sequences were isolated by PCR using primers based on the B73 *Zmtps21* and Mo17 *ZmTps21* genome sequences (Supplemental Table S1). Sequence analyses demonstrated that the *Zmtps21* alleles from B73-like lines (Ki3, M37W, MS71, M162W, CML247, Ki11, and Mo18W) share greater than 98% DNA sequence identity and basic genome structure, whereas Mo17-like *ZmTps21* alleles (Hp301, TX303, Oh43, Oh7B, Ky21, and W22) contain six exons and share greater than 98% sequence identity at the amino acid level (Supplemental Figs. S5 and S6). These results support the hypothesis that B73-like inbred lines share a common mutation ancestry.

#### In Vitro Assays Demonstrate That *ZmTps21* Is a Largely Product-Specific $\beta$ -Selinene Synthase

*ZmTps21* lacks a predicted N-terminal transit peptide, suggesting that the enzyme is not targeted to plastids, as is typical of monoterpene and diterpene synthases, but instead remains cytosolic, consistent with predictions for a sesquiterpene synthase (Gershenzon and Kreis, 1999). To obtain additional support for the hypothesis that Mo17 *ZmTps21* is a  $\beta$ -selinene synthase, heterologous expression was performed in *E. coli* and the resulting protein extract was incubated with the precursor substrate FPP.  $\beta$ -Selinene is the dominant product observed by GC-MS along with several other minor sesquiterpene olefins, including  $\alpha$ -selinene and  $\beta$ -elemene (Fig. 4). Thus, *ZmTps21* encodes a selinene synthase with predominant  $\beta$ -selinene product specificity that includes  $\alpha$ -selinene as a minor product, consistent with the olefin

#### Figure 2. (Continued.)

with five individual third instar larvae where distributions were measured at 30, 60, 90, 120, 180, and 240 min and collectively averaged (Student's *t* test,  $P > 0.05$ ). L, Average ( $n \geq 5$ ,  $\pm$ SE) performance (percentage relative weight gain) of third instar WCR and *D. balteata* larvae over 2 d of feeding on root tissues with (+) and without (–) additions of  $\beta$ -costic acid as described in the preference study (two-way ANOVA,  $P < 0.05$ ).

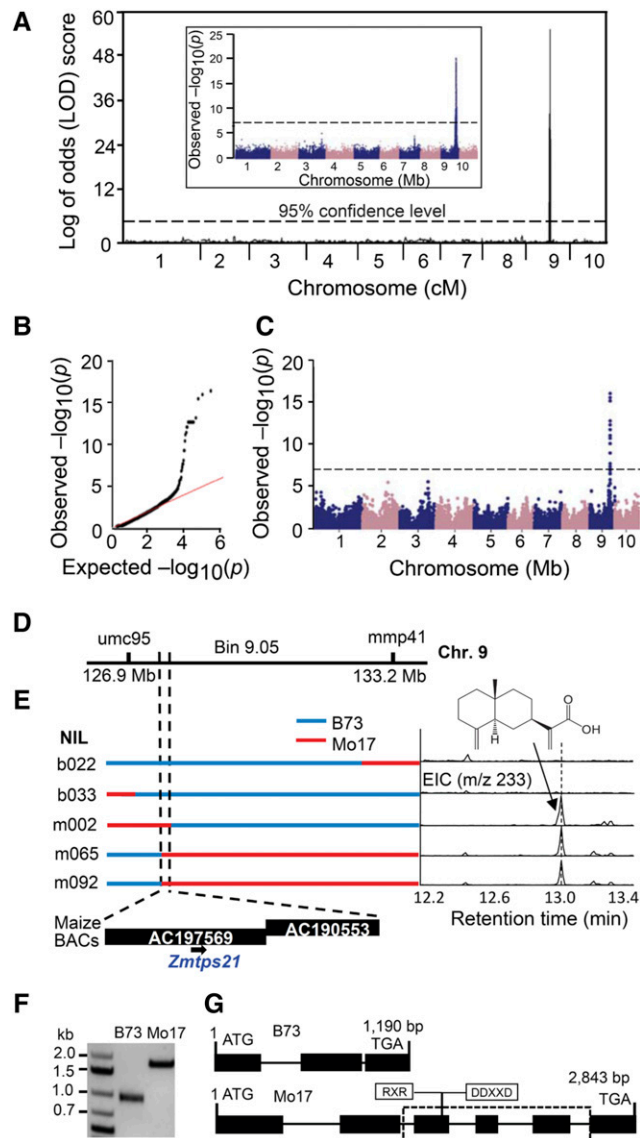


**Figure 3.** Combined linkage and association mapping identifies *ZmTps21* as a candidate  $\beta$ -selinene synthase. A, Major mQTL for  $\beta$ -costic acid production detected on chromosome 9 by CIM using IBM RILs. The inset shows comparative association analysis of the IBM RIL  $\beta$ -costic acid levels using the GLM and 173,984 SNPs. The most statistically significant SNP is located at position 127,854,265 on chromosome 9 (B73 RefGen\_v2), with the dashed line denoting the 5% Bonferroni correction. cM, Centimorgan. B, Quantile-quantile plot for the association analysis of  $\beta$ -costic acid levels in the Goodman diversity panel. C, Manhattan plot of the association analysis (MLM) of  $\beta$ -costic acid levels in replicate 1 of the Goodman diversity panel following 3 d of fungal elicitation. The dashed line denotes the 5% Bonferroni-corrected threshold for 246,477 SNP markers, with the most statistically significant SNP located at position 127,858,963 (B73 RefGen\_v2) on chromosome 9. D, Location of the candidate gene *ZmTps21* on the physical map supported by both linkage analysis and association analysis. E, Fine-mapping with IBM NILs; B73 and Mo17 chromosomal segments are represented by blue and red, respectively.  $\beta$ -Costic acid chemotypes of IBM NILs are indicated as GC/EI-MS traces ( $m/z = 233$ ). F, Agarose gel PCR-amplified products demonstrate a cDNA length polymorphism between B73 *ZmTps21* and Mo17

and oxygenated metabolite ratios observed in planta (Fig. 1; Supplemental Fig. S1). Injection of the *ZmTps21* reaction products on a GC column at different temperatures revealed that the  $\beta$ -elemene present is due to a Cope rearrangement of germacrene A (Supplemental Figs. S7 and S8; de Kraker et al., 2001). Germacrene A also is a neutral reaction intermediate of the tobacco (*Nicotiana tabacum*) enzyme 5-*epi*-aristolochene synthase (TEAS) responsible for the pathogen-elicited biosynthesis of capsidiol (Cane, 1990; Starks et al., 1997). The enzymatic protonation of germacrene A leads to the eudesmane carbocation being further converted to 5-*epi*-aristolochene. Given that  $\beta$ -selinene is simply formed by a deprotonation of a eudesmane carbocation, it likely that the reaction catalyzed by *ZmTps21* also includes the formation and protonation of germacrene A. A sequence comparison of *ZmTps21* with TEAS and other Tps able to protonate neutral reaction intermediates demonstrates that the amino acids of the catalytic triad involved in the protonation reaction are conserved (Starks et al., 1997; Supplemental Fig. S4). Curiously, two *ZmTps21* mutants with altered C termini obtained as cloning artifacts produced only germacrene A (Supplemental Figs. S7 and S8), suggesting additional influence of the C terminus on the protonation reaction and specificity of the final product.

### *ZmTps21* Transcripts Are Pathogen Inducible and Correspond with $\beta$ -Costic Acid Accumulation

To examine endogenous patterns, we compared Mo17 *ZmTps21* expression with established *ZmTps6/11* expression associated with zealexin biosynthesis (Köllner et al., 2008b; Huffaker et al., 2011). Similar to *ZmTps6/11*-zealexin relationships, *ZmTps21* transcripts and  $\beta$ -costic acid are barely detectable in control tissues and are not elicited significantly by mechanical damage alone (Fig. 5). After elicitation with heat-killed *Fusarium* spp. hyphae, *ZmTps6/11* transcripts reached maximal levels at day 1, while *ZmTps21* transcript levels continued to accumulate for an additional 1 d (Fig. 5). Zealexin A1 was readily detectable at day 1 and continued to increase over the 4 d, while  $\beta$ -costic acid accumulation was first detected at day 2 and reached similar levels at day 4 (Fig. 5). Thus, *ZmTps21* transcripts and product accumulation display longer term and temporally layered elicitation kinetics alongside the zealexin biosynthetic pathway.

To examine whether *ZmTps21* transcripts and  $\beta$ -costic acid levels change specifically in response to aggressive pathogens such as *C. heterostrophus* and *F. verticillioides* or whether the response also follows opportunistic fungi such as *Rhizopus microsporus* and

*ZmTps21*. G, Diagrammatic structures of B73 *ZmTps21* and Mo17 *ZmTps21* genes based on sequencing. Exons and introns are denoted as rectangular bars and black lines, respectively. The dashed rectangle indicates the missing B73 genomic DNA and the relative positions of encoded conserved RXR and DDXXD motifs for terpene cyclase activity.

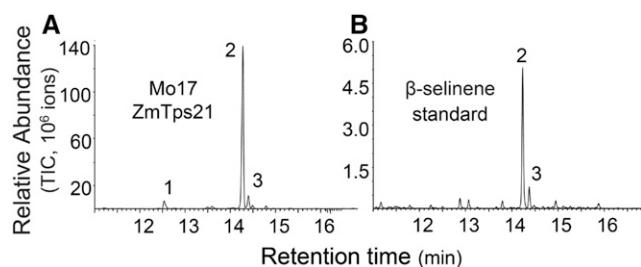


**Figure 4.** Mo17 *ZmTps21* encodes a functional  $\beta$ -selinene synthase. A, Mo17 *ZmTps21* was heterologously expressed in *E. coli*, and the resulting protein extract was incubated with (*E,E*)-FPP. Mo17 *ZmTps21* products were collected using solid-phase microextraction (SPME) and analyzed by GC-MS, revealing  $\beta$ -selinene (2) as the dominant product, with lower yet detectable levels of  $\beta$ -elemene (germacrene A rearrangement product); (1) and  $\alpha$ -selinene (3). B, Celery (*Apium graveolens*) fruit essential oil was used as a natural product standard for  $\beta$ -selinene: $\alpha$ -selinene (9:1). TIC, Total ion chromatograms.

*Aspergillus parasiticus*, both parameters were analyzed in inoculated stems. Exposure to *C. heterostrophus*, *F. verticillioides*, *R. microsporus*, and *A. parasiticus* all resulted in significant induction of both *ZmTps6/11* transcript levels and zealexin A1, which vary in response to different fungi (Fig. 5; Huffaker et al., 2011). In the same context, the four fungal species also led to significant accumulation of *ZmTps21* transcripts and  $\beta$ -costic acid (Fig. 5). Infection with *C. heterostrophus* led to the highest induction of both *ZmTps21* transcripts and  $\beta$ -costic acid in stems, similar to *ZmTps6/11* transcripts and zealexin levels, respectively (Fig. 5). To further consider the natural occurrence of  $\beta$ -selinene-derived metabolites in diverse inbreds (McMullen et al., 2009b), we analyzed the scutella tissues of 10-d-old seedling plants.  $\beta$ -Costic acid was detected in all lines harboring Mo17-like *ZmTps21* alleles (Hp301, TX303, Oh43, Oh7B, Ky21, and W22) and was comparatively absent from all inbreds harboring B73-like *Zmtps21* (Ki3, M37W, MS71, M162W, CML247, Ki11, and Mo18W) pseudogenes (Fig. 5; Supplemental Figs. S5 and S6). Collectively, these results support the existence of a single  $\beta$ -selinene synthase in maize responsible for the production of  $\beta$ -costic acid.

#### In Vitro and in Vivo Assays Support a Defensive Role for $\beta$ -Costic Acid in Fungal Disease Resistance

In an effort to assess physiological roles, we quantified  $\beta$ -costic acid present in replications of field-collected roots of B73, sweet corn (variety Golden Queen), Mo17, and the *ZmTps21* IBM RIL 0287. On average, sectors of roots containing visible necrosis from each responsive line contained well over 100  $\mu\text{g g}^{-1}$  fresh weight  $\beta$ -costic acid (Fig. 5). Using this conservative baseline, we then examined the antimicrobial activity of  $\beta$ -costic acid against *F. verticillioides*, *F. graminearum*, *R. microsporus*, *A. parasiticus*, and *C. heterostrophus* in liquid culture assays. At 100  $\mu\text{g mL}^{-1}$ ,  $\beta$ -costic acid completely

inhibited the growth of *R. microsporus* and significantly suppressed the growth of all other fungi (Fig. 6; Supplemental Fig. S9). Importantly,  $\beta$ -costic acid concentrations as low as 25  $\mu\text{g mL}^{-1}$  retained significant inhibitory activity, in each case demonstrating that  $\beta$ -costic acid has the potential to function as wide-spectrum antifungal defense at low doses. To estimate in vivo roles, mature roots of greenhouse-grown B73, Mo17, and two predominantly Mo17 IBM NILs (Supplemental Fig. S9) were damaged and treated with either water or water containing spores of *F. verticillioides* and *F. graminearum* separately. Seven days later, the B73 inbred and the IBM NIL (m050) harboring a *Zmtps21* pseudogene displayed significantly greater levels of disease as estimated by *Fusarium* spp. DNA levels compared with Mo17 and the functional *ZmTps21* IBM NIL (m065; Fig. 6). Collectively, our results are consistent with *ZmTps21* pathway products as mediators of antifungal defenses.

#### DISCUSSION

Maize biochemicals either demonstrated or predicted to mediate insect and pathogen defense include diverse volatiles (Degenhardt, 2009; Degenhardt et al., 2009a), benzoxazinoids (Frey et al., 2009; Ahmad et al., 2011; Meihls et al., 2013; Handrick et al., 2016), flavonoids and C-linked flavonoid glycosides (Meyer et al., 2007; Balmer et al., 2013; Casas et al., 2016), nonprotein amino acids (Yan et al., 2015), oxylipins (Christensen et al., 2015; Borrego and Kolomiets, 2016), and nonvolatile terpenoids (Schmelz et al., 2014). Among all biosynthetic classes, terpenoids are the most diverse structurally and in demonstrated breadth of ecological interactions mediated (Gershenson and Dudareva, 2007). At the genome level, plants commonly possess midsized terpene synthase gene families ranging from 14 to 70 members (Chen et al., 2011). More specifically, in maize, the use of terpene as a keyword search in Phytozome (<https://phytozome.jgi.doe.gov>) currently reveals more than 30 *Tps* gene models. Collective efforts have resulted in the genetic, biochemical, and ecological characterization of approximately half of the maize enzymes encoded by *Tps* with product specificity in the production of monoterpenes, sesquiterpenes, and diterpenes (Schnee et al., 2002, 2006; Köllner et al., 2004b, 2008a; Degenhardt et al., 2009; Fu et al., 2016; Richter et al., 2016). Maize terpene volatiles are often highly inducible following insect attack and aid in the attraction of diverse natural enemies both aboveground and belowground (Turlings et al., 1990; Rasmann et al., 2005; Degenhardt et al., 2009a). Oxygenated nonvolatile terpenoids also can accumulate and act as antifungal agents and insect antifeedants (Schmelz et al., 2011). As part of this biochemical complexity, we demonstrate that maize tissues are capable of accumulating both high levels of the sesquiterpene olefin  $\beta$ -selinene and the corresponding nonvolatile oxygenated derivative termed  $\beta$ -costic acid. Intriguingly,  $\beta$ -costic acid is

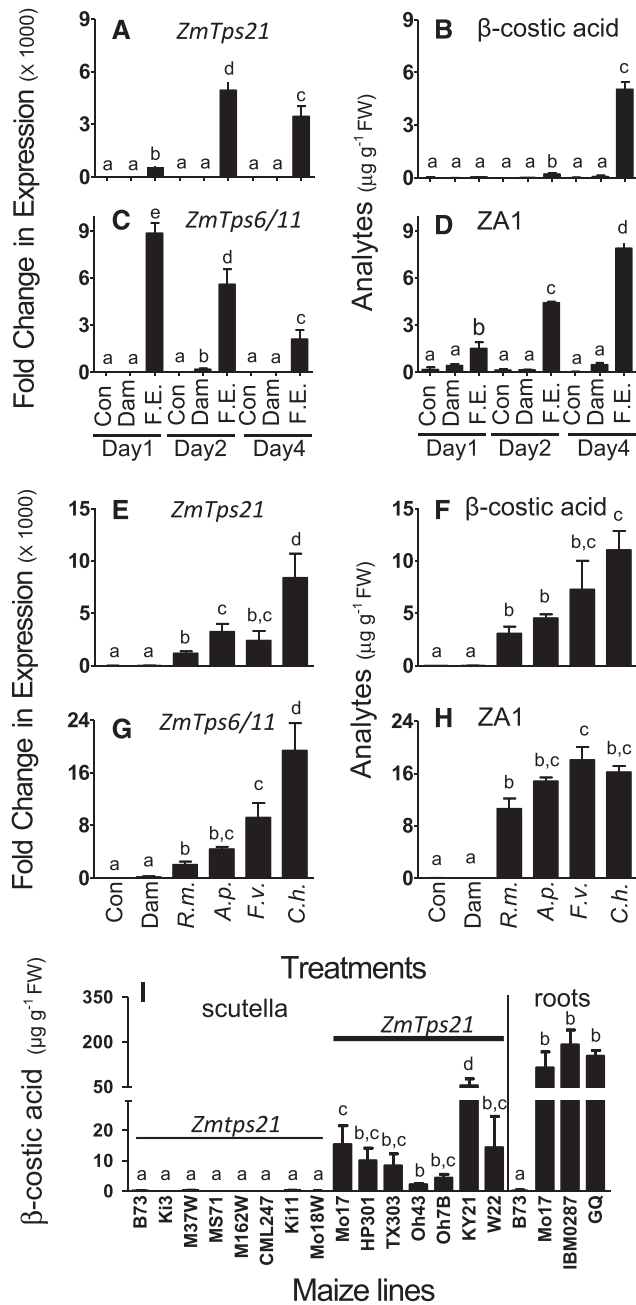


**Figure 5.** *ZmTps21* transcripts are elicited by diverse fungi and precede β-costic acid accumulation detectable in diverse maize lines. A to D, Average (n = 4; ±SE) Mo17 *ZmTps21* (A), β-costic acid (B), *ZmTps6/11* (C), and zealexin A1 (D) as quantitative reverse transcription (qRT)-PCR fold changes of transcripts and corresponding phytoalexin concentrations (µg g<sup>-1</sup> fresh weight [FW]) in intact control stems (Con) or those damaged and treated with either water (Dam) or a heat-killed *Fusarium* spp. elicitor (F.E.) hyphae preparation after 1, 2, or 4 d. E to H, Average (n = 4; ±SE) Mo17 *ZmTps21* (E), β-costic acid (F), *ZmTps6/11* (G), and zealexin A1 (H) as qRT-PCR fold changes of transcripts and corresponding phytoalexin concentrations (µg g<sup>-1</sup> fresh weight) in intact control stems or those damaged and treated with either 100 µL of water alone or spore suspensions (1 × 10<sup>7</sup> mL<sup>-1</sup>) of *R. microsporus* (*R.m.*), *A. parasiticus* nor-1 (*A.p.*), *F. verticillioides* (*F.v.*), or *C. heterostrophus* (*C.h.*) and harvested at 2 and 4 d for transcripts and metabolites,

produced in diverse aromatic and medicinal plants widely investigated for bioactive agents driving antibiotic and antiarthropod activities (Rao and Alvarez, 1981; Wu et al., 2006; Katerinopoulos et al., 2011). Despite their widespread occurrence in nature, Tps essential for the specific *in vivo* production of β-costic acid have not been demonstrated previously in planta. Here, we describe a maize β-selinene synthase, termed *ZmTps21*, that is required for the inducible accumulation of β-costic acid.

High tissue concentrations of β-costic acid were first detected in mature field-collected roots of both sweet corn and Mo17 but appeared absent from the B73 inbred. The use of complementary mapping resources and the induced production of β-costic acid as a qualitative trait demonstrated a single narrow QTL containing a *Tps* gene candidate.

To examine the full-length Mo17 *ZmTps21* allele identified, heterologous expression experiments were conducted in *E. coli*, and protein extracts incubated with FPP yielded β-selinene as the dominant volatile product. Based on numerous inbred lines and predicted proteins from genome sequences (Supplemental Figs. S5 and S6), the *in vitro* products of functional *ZmTps21* are consistent with the endogenous presence of β-costic acid in all Mo17-like *ZmTps21* lines and likewise an absence in all B73-like *ZmTps21* lines (Fig. 5). Precursors of dominant biochemical defense pathways are commonly the products of fully functional duplicate genes (Köllner et al., 2008b; McMullen et al., 2009a); however, mGWAS mapping results (Fig. 2) and the exclusive presence of β-costic acid (Fig. 5) in lines with full-length *ZmTps21* alleles collectively support the existence of a single maize β-selinene synthase. At the enzymatic level, the existence of a product-specific β-selinene synthase was first reported in 1992 through the examination of *Citronella mitis* fruits; however, the specific Tps gene responsible remains unknown (Belingeri et al., 1992). Acid-induced cyclization of germacrene also can yield selinenes, making it highly probable that a germacrene A synthase is responsible for the costol, costal, and costic acid eudesmanes in costus root oil; however, it remains unknown if costus contains a specific β-selinene synthase (de Kraker et al., 2001). Further elucidation of the β-costic acid pathway will require the discovery of a yet unresolved cytochrome P450 monooxygenase(s) performing sequential oxidations leading to the carboxylic acid. Characterized germacrene A oxidases from the Asteraceae drive the biosynthesis of germacrene A acid,

respectively. I, Average (n = 4; ±SE) β-costic acid concentrations (µg g<sup>-1</sup> fresh weight) in the scutella of 10-d-old maize seedlings from 15 inbred maize lines and mature field-collected roots displaying necrosis. Hybrids include sweet corn (variety Golden Queen [GQ]) and IBM-RIL-0287. Within plots, different letters (a–e) represent significant differences (all ANOVA, P < 0.05; Tukey’s test corrections for multiple comparisons, P < 0.05).



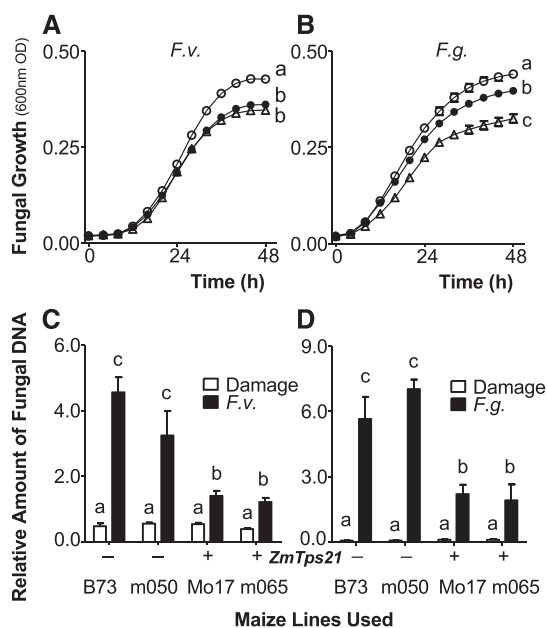


**Figure 6.** *ZmTps21*-derived products inhibit *Fusarium* spp. fungi in vitro and correspond with improved disease resistance in vivo. A and B, Average ( $n = 8$ ;  $\pm$ SE) fungal growth estimates (600-nm OD) of *F. verticillioides* (*F.v.*; A) and *F. graminearum* (*F.g.*; B) in liquid medium in the presence of  $\beta$ -costic acid at 0 (white circles), 25 (black circles), and 100 (triangles)  $\mu\text{g mL}^{-1}$ . C and D, Average ( $n = 4$ ;  $\pm$ SE) ratio of fungal DNA-to-plant DNA levels present in maize roots 7 d after damage and inoculation with 100  $\mu\text{L}$  of either water or  $1 \times 10^7$  conidia  $\text{mL}^{-1}$  *F. verticillioides* (C) and *F. graminearum* (D) in B73, Mo17, and IBM NILs harboring active (+; m065) and inactive (–; m050) alleles of *ZmTps21*. Within plots, different letters (a–c) represent significant differences (all ANOVA,  $P < 0.05$ ; Tukey's test corrections for multiple comparisons,  $P < 0.05$ ).

which, following acid-induced rearrangement, can yield blends that include  $\beta$ -costic acid (Nguyen et al., 2010). A related P450 that directly oxidizes  $\beta$ -selinene to yield  $\beta$ -costic acid is predicted to occur in maize yet remains unknown.

While numerous plants in nature constitutively make  $\beta$ -selinene in specific tissues and life stages,  $\beta$ -selinene is rarely detected in maize and has occurred only in the context of pathogen attack (Becker et al., 2014; Sowbhagya, 2014). Consistent with this observation, we find *ZmTps21* transcripts largely undetectable in healthy control tissues or those experiencing simple mechanical damage (Fig. 5). In contrast, heat-killed *Fusarium* spp. hyphae and a wide range of live fungal species elicit *ZmTps21* transcript accumulation and  $\beta$ -costic acid production. With conceptual similarities to the zealexin pathway, the elicitation kinetics of both *ZmTps21* transcripts and  $\beta$ -costic acid differ and are temporally behind those of *ZmTps6/11* and zealexins. Given the broader range of fungus species displaying  $\beta$ -costic acid-mediated growth suppression at 25  $\mu\text{g mL}^{-1}$  compared with similar assays using zealexins (Huffaker et al., 2011), it is possible that the *ZmTps21* pathway exists as an additional potent line of defense

activated sequentially as maize plants experience sustained attack. If this hypothesis is true, related studies on maize disease resistance should note biological roles for QTLs that include *ZmTps21*. Supportively, independent disease-related QTLs have been detected in broad regions spanning bin 9.05 (Baumgarten et al., 2007; Berger et al., 2014). More specifically, *ZmTps21* (GRMZM2G011151) has been identified as uniquely present in transcriptome analyses of resistant inbred lines associated with enhanced antifungal defenses (Lanubile et al., 2014). In an empirical assessment of the in vivo role of *ZmTps21*-derived defenses, root experiments using B73, Mo17, and two Mo17 NILs support the suppression of both *F. graminearum* and *F. verticillioides* growth in lines carrying functional Mo17 *ZmTps21* alleles (Fig. 6). Most maize biochemical defenses likely function in the context of complex arrays of bioactive metabolites from numerous pathways. In this context, isogenic mutants in numerous inbred backgrounds would be an ideal and improved platform for the critical examination of *ZmTps21*-mediated biological functions. While this study does not accomplish this long-term goal, we provide a foundation and mechanistic justification for related research directions.

Curiously, of lines closely examined at the gene level,  $\beta$ -costic acid biosynthesis mediated by *ZmTps21* is associated with inbreds originating from U.S. breeding programs. In contrast,  $\beta$ -costic acid biosynthetic capacity is largely absent from more geographically diverse accessions. It is tempting to speculate that, while the  $\beta$ -costic acid pathway is commonly absent due to a partial gene deletion, *ZmTps21* may have been maintained by positive selection during the breeding of U.S. maize lines. WCR larvae exist as a candidate pest pressure known to devastate the roots of temperate maize through belowground herbivory and the promotion of secondary disease (Flint-Garcia et al., 2009; Gray et al., 2009). In growth chamber experiments, maize plants containing a functional *ZmTps21* allele produced both  $\beta$ -selinene and  $\beta$ -costic acid following damage by WCR larvae (Fig. 2). Consistent with a long-term association, unlike the generalist *D. balteata*, WCR larvae were not significantly affected in preference or performance by  $\beta$ -costic acid as a direct defense (Fig. 2). In this context,  $\beta$ -costic acid is likely to be more important in limiting the secondary spread of fungal pathogens promoted by root herbivory. However, while not examined specifically here, we speculate that root pools of  $\beta$ -selinene may serve as a volatile attractant to natural enemies of *Diabrotica* spp. larvae such as entomopathogenic nematodes (Rasmann et al., 2005; Degenhardt et al., 2009a). This phenomenon has been demonstrated in the context of trace amounts of maize root caryophyllene elicited following WCR larval herbivory. More broadly, numerous root terpene volatiles can attract both entomopathogenic and phytopathogenic nematodes, a result that highlights complex tradeoffs in the deployment of rhizosphere signals (Ali et al., 2011).

In conclusion, this study identifies the presence of numerous  $\alpha/\beta$ -selinene-derived metabolites in maize tissues following biotic stress. In numerous trials using select maize lines,  $\beta$ -selinene and  $\beta$ -costic acid exist as predominant ZmTps21-derived terpenoids produced following fungal elicitation, long-term root herbivory, and combined field pressures. Antifungal assays using both *in vitro* and *in vivo* approaches support an anti-fungal defense role for ZmTps21 pathway products. Root herbivores are likely to be additionally impacted given that  $\beta$ -costic acid can reduce the performance of generalists such as *D. balteata* in controlled bioassays. The discovery of further immune-related biochemical traits is certain to continue, given the extreme genetic diversity in maize highlighted by over 8,000 representative transcript assemblies detectable in diverse germplasm that are absent from B73 (Hirsch et al., 2014). To fill existing voids highlighted by comparative genomics, the combined application of metabolomics, mapping, and *in vitro* biochemistry provides a useful approach to rapidly connect phenotypes with genotypes (Meihls et al., 2013; Handrick et al., 2016; Richter et al., 2016). Our current identification of ZmTps21 as a  $\beta$ -selinene synthase required for  $\beta$ -costic acid production adds to the foundational knowledge of useful maize biochemical pathways that can be combined intentionally to combat complex biotic pressures.

## MATERIALS AND METHODS

### Plant and Fungal Materials

Seeds of the maize (*Zea mays*) IBM population of RILs and the Goodman diversity panel (Flint-Garcia et al., 2005) were kindly provided by Dr. Peter Balint-Kurti (U.S. Department of Agriculture-Agricultural Research Service [USDA-ARS]) and Dr. Georg Jander (Boyce Thompson Institute; Supplemental Table S2). The IBM RILs and Goodman diversity panel (replicate 2) were planted at the Biology Field Station located on the University of California San Diego campus in La Jolla, California, during the summers of 2015 and 2016, respectively. Field-challenged roots from B73, Mo17, hybrid sweet corn (variety Golden Queen; Southern States Cooperative), and IBM RILs were recovered 70 d after planting, washed, frozen in liquid N<sub>2</sub>, ground to a fine powder, and ultimately used for genetic mapping. Seeds of indicated B73 × Mo17 NILs (provided by the Maize Genetic COOP Stock Center) and landrace inbreds (B73, Ki3, M37W, Ms71, M162W, CML247, Ki11, Mo18W, Hp301, TX303, Oh43, Oh7B, Ky21, Mo17, and W22; National Genetic Resources Program, Germplasm Resources Information Network) were germinated in MetroMix 200 (Sun Gro Horticulture) supplemented with 14-14-14 Osmocote (Scotts Miracle-Gro) and grown in a greenhouse as described previously (Schmelz et al., 2009; Supplemental Table S2). Fungal stock cultures of *Rhizopus microsporus* (Northern Regional Research Laboratory [NRRRL] stock no. 54029), *Fusarium verticillioides* (NRRRL stock no. 7415), *Fusarium graminearum* (NRRRL stock no. 31084), *Aspergillus parasiticus* nor-1, and *Cochliobolus heterostrophus* were grown on V8 agar for 12 d before the quantification and use of spores (Huffaker et al., 2011, 2013). Heat-killed *Fusarium venenatum* (strain PTA-2684) hyphae was commercially obtained (Monde Nissin) and used safely for large-scale field mGWAS trials as a noninfectious elicitor lacking known *Fusarium* spp. mycotoxins.

### Genetic Mapping of ZmTps21

Using the presence of  $\beta$ -costic acid in necrotic tissues as a trait, the B73 *ZmTps21* locus was mapped using 216 IBM RILs (Lee et al., 2002) and further supported using select B73 × Mo17 NILs (Eichten et al., 2011). Marker data for the IBM RIL population were provided by Dr. Peter Balint-Kurti. Windows

QTL Cartographer (version 2.5; <http://statgen.ncsu.edu/~shchwang/WQTL.Cart.htm>) was employed for mQTL analysis with CIM. The WinQTL-Cart program was set as follows: CIM program module = model 6, standard model; walking speed = 1 centimorgan; control marker numbers = 5; window size = 10 centimorgan; regression method = backward regression. Permutations (500) were run to determine the  $P < 0.05$  logarithm (base 10) of odds significance threshold (Churchill and Doerge, 1994). A list of RILs and NILs used for mapping in this study is given in Supplemental Table S2. In an effort to confirm and potentially refine the position of the mQTLs identified using CIM, association analyses also were conducted on the IBM RILs using the GLM in TASSEL 5.0 (Bradbury et al., 2007) and the unified MLM to effectively control for false positives arising from the differential population structure and familial relatedness present in diversity panels (Yu et al., 2006). Unlike diversity panels, differential population structure and familial relatedness are not typically significant features in biparental RIL panels; thus, the GLM and MLM were predicted to generate similar results in the IBM RIL association analyses. Genotypic data from imputed IBM RIL SNP markers (July 2012 All *Zea* GBS final build; [www.panzea.org](http://www.panzea.org)) were used for association analyses of root  $\beta$ -costic acid levels in the IBM population. A total of 173,984 SNP markers with less than 20% missing genotypes and minor allele frequency greater than 15% were used.

An mGWAS was conducted for elicited levels of  $\beta$ -costic acid as a trait in the Goodman diversity panel (Flint-Garcia et al., 2005) using the unified MLM in TASSEL 5.0 (Yu et al., 2006; Bradbury et al., 2007). Final analyses were conducted with the R package GAPIT (Zhang et al., 2010; Lipka et al., 2012), which involves EMMA (executed by R package) and compressed MLM population parameters determined previously to identify genomic regions putatively associated with the trait. GWAS analyses utilized a B73 version 2 referenced HapMap consisting of 246,477 SNPs derived previously from an Illumina 50K array (Cook et al., 2012) and a genotyping-by-sequencing strategy (Elshire et al., 2011) filtering less than 20% missing genotype data with minor allele frequency greater than 5% (Samayoa et al., 2015; Olukolu et al., 2016). The kinship matrix (K), estimated from 246,477 SNPs, was used jointly with population structure (Q) to improve association analysis (VanRaden, 2008). All metabolite data were log<sub>2</sub> transformed prior to statistical analysis to improve normality. The quantile-quantile plots and Manhattan plots were constructed in the R package qqman (<http://cran.r-project.org/web/packages/qqman/>; Turner, 2014).

### Identification and Quantification of Metabolites

Unless stated otherwise, all maize tissue samples were rinsed with water, frozen in liquid N<sub>2</sub>, ground to a fine powder in a mortar, and stored at  $-80^{\circ}\text{C}$  for further analyses. For vapor phase extraction-based sample preparation, 50-mg aliquots were first weighed, solvent extracted in a bead homogenizer, and derivatized using trimethylsilyldiazomethane as described previously (Schmelz et al., 2004, 2011). GC-MS analysis was conducted using an Agilent 6890 series gas chromatograph coupled to an Agilent 5973 mass selective detector (interface temperature,  $250^{\circ}\text{C}$ ; mass temperature,  $150^{\circ}\text{C}$ ; source temperature,  $230^{\circ}\text{C}$ ; electron energy, 70 eV). The gas chromatograph was operated with a DB-35MS column (Agilent; 30 m × 0.25 mm × 0.25  $\mu\text{m}$ ). The sample was introduced as a splitless injection with an initial oven temperature of  $45^{\circ}\text{C}$ . The temperature was held for 2.25 min, then increased to  $300^{\circ}\text{C}$  with a gradient of  $20^{\circ}\text{C min}^{-1}$ , and held at  $300^{\circ}\text{C}$  for 5 min. GC/EI-MS based quantification of  $\beta$ -costic acid was based upon the slope of an external standard curve constructed from  $\beta$ -costic acid (Ark Pharm; no. AK168379) spiked into 50-mg aliquots of frozen powdered untreated maize stem tissues, which were then processed using vapor phase extraction (Schmelz et al., 2004). In representative samples analyzed by GC/EI-MS,  $\beta$ -costol was identified based on a 99% EI match within the Robert P. Adams Essential Oil MS library (Allured Books). While not detected previously in maize,  $\beta$ -costol is an anticipated intermediate in samples rich in both  $\beta$ -selinene and  $\beta$ -costic acid.

For headspace recovery of ZmTps21 enzyme products by SPME, fibers coated with 100  $\mu\text{m}$  polydimethylsiloxane (Supelco) were placed into reaction vials for 60-min incubations at  $30^{\circ}\text{C}$  and then introduced into the gas chromatograph injector for the analyses of the adsorbed reaction products. GC-MS analyses conducted on SPME samples utilized a splitless injection, a DB-5MS column (Agilent; 30 m × 0.25 mm × 0.25  $\mu\text{m}$ ), and an initial oven temperature of  $80^{\circ}\text{C}$ . The temperature was held for 2 min, then increased to  $240^{\circ}\text{C}$  with a gradient of  $7^{\circ}\text{C min}^{-1}$ , increased further to  $300^{\circ}\text{C}$  with a gradient of  $60^{\circ}\text{C min}^{-1}$ , and held of 2 min. Precise instrument settings of the Agilent 5973 mass selective detector were identical to those stated above used for plant samples. For GC-MS analysis with a cooler injector, the injector temperature was reduced from  $240^{\circ}\text{C}$  to  $150^{\circ}\text{C}$ .

Volatiles emitted from elicited stems and naturally challenged roots of field-grown plants were collected by passing purified air over the tissue samples at 600 mL min<sup>-1</sup> and trapped on inert filters containing 50 mg of HayeSep Q (80- to 100- $\mu$ m mesh) polymer adsorbent (Sigma-Aldrich). Individual samples were then eluted with 150  $\mu$ L of methylene chloride and analyzed by GC-FID as described previously (Schmelz et al., 2001).  $\beta$ -Selinene and related volatiles were quantified by GC-FID using the slope of an external standard curve of (*E*)- $\beta$ -farnesene. Select samples were analyzed by GC/EI-MS to confirm individual peak identities of representative replicates. This included the comparison of retention times with authentic standards and comparison of mass spectra with the Wiley, National Institute of Standards and Technology, and Adams libraries.

To ensure maximal independence of the second GWAS replicate that was grown in the field, analytical conditions utilized liquid chromatography-MS instead of GC-MS. Reacted stem tissues were first ground to a fine powder with liquid N<sub>2</sub> and weighed out in 50-mg aliquots. Tissue samples were sequentially and additively bead homogenized in (1) 100  $\mu$ L of 1-propanol:acetonitrile:formic acid (1:1:0.01), (2) 250  $\mu$ L of acetonitrile:ethyl acetate (1:1), and (3) 100  $\mu$ L of water. Each combined sample consisted of a comiscible acidified solvent mixture of primarily 1-propanol:acetonitrile:ethyl acetate:water in the approximate proportion of 11:39:28:22, which was then centrifuged at 15,000 rpm for 20 min. Approximately 150  $\mu$ L of the particulate free supernatant was carefully removed for liquid chromatography-MS automated sample analyses utilizing 5- $\mu$ L injections. The liquid chromatograph consisted of an Agilent 1260 Infinitely Series HiP Degasser (G4225A), 1260 binary pump (G1312B), and 1260 autosampler (G1329B). The binary gradient mobile phase consisted of 0.1% (v/v) formic acid in water (solvent A) and 0.1% (v/v) formic acid in methanol (solvent B). Analytical samples were chromatographically separated on a Zorbax Eclipse Plus C18 Rapid Resolution HD column (Agilent; 1.8  $\mu$ m, 2.1  $\times$  50 mm) using a 0.35 mL min<sup>-1</sup> flow rate. The mobile phase gradient was as follows: 0 to 2 min, 5% B constant ratio; 3 min, 24% B; 18 min, 98% B; 25 min, 98% B; and 26 min, 5% B for column reequilibration before the next injection. Eluted analytes underwent electrospray ionization via an Agilent Jet Stream Source with thermal gradient focusing using the following parameters: nozzle voltage (500 V), N<sub>2</sub> nebulizing gas (flow, 12 L min<sup>-1</sup>, 55 p.s.i., 225°C), and sheath gas (350°C, 12 L min<sup>-1</sup>). The transfer inlet capillary was 3,500 V, and both MS1 and MS2 heaters were at 100°C. Negative ionization [M-H]<sup>-</sup> mode scans (0.1-atomic mass unit steps, 2.25 cycles s<sup>-1</sup>) from *m/z* 100 to 1,000 were acquired. After considerable unsuccessful attempts to optimize parameters required to obtain meaningful daughter ion fragments from  $\beta$ -costic acid, analyses relied exclusively on the native parent [M-H]<sup>-</sup> ion *m/z* 233 and stable retention time of 16.65 min separated from established maize zealexins. Quantification utilized an external standard curve of  $\beta$ -costic acid (Ark Pharm; no. AK168379) analyzed under identical conditions.

## Controlled Maize Elicitation Assays

Controlled maize elicitation assays used 30- to 40-d-old greenhouse plants grown in 1-L plastic pots or, in the case of the Goodman diversity panel (second replicate), field-grown plants. Plants in damage-related treatment groups were slit in the center, spanning both sides of the stem, with a surgical scalpel that was pulled 8 to 10 cm upward to create a parallel longitudinal incision. The treatment spanned the upper nodes, internodes, and the most basal portion of unexpanded leaves. All fungal spore inoculation (1  $\times$  10<sup>7</sup> mL<sup>-1</sup>) treatments were performed in 100  $\mu$ L of water. For experiments involving stem elicitation with heat-killed *Fusarium* spp. hyphae, crude material was homogenized in a Waring blender at maximum speed for 3 min in the presence of additional water at 20% to 30% (w/w) to create a thick smooth paste. Approximately 500  $\mu$ L of crude elicitor was introduced into each slit stem followed by sealing the site with clear plastic packing tape to minimize desiccation of the treated stem tissues. For each individual experiment, details relating to specific tissues, biological replications, and harvest time points are noted in the figures and captions.

For the assay of plant responses to long-term WCR (*Diabrotica virgifera virgifera*) herbivory, seeds of an IBM line carrying a functional *ZmTps21* gene (IBM-RIL-0287) were grown in 946-mL DM32R cups (Dart Container) filled with greenhouse potting medium and fertilized following Gassmann et al. (2011). Seeds were planted 1 month prior to WCR inoculation and maintained at 23°C to 28°C in a greenhouse with supplemental daylight balanced illumination on a 16/8-h (light/dark) photoperiod. Plants were watered daily as needed to prevent saturated soil conditions. Inoculation and care of V5-V6 stage or greater (Abendroth, 2011) treated plants followed Gassmann et al. (2011). Cups were inoculated with *n* = 10 neonate WCR larvae (obtained from USDA-ARS-NCARL) and held in an incubator at 24°C with 40% to 60% relative humidity and

watered sparingly as needed to minimize pot flooding. The experiment utilized four replicates per treatment. After 17 d, 1-g samples of insect-attacked and healthy root tissues were collected from the plants, frozen on dry ice, and stored for chemical analyses.

## *Diabrotica* spp. Preference and Performance Assays

For studies on preference and performance, WCR eggs and *Diabrotica balteata* (LeConte) eggs were obtained from USDA-ARS-NCARL and Syngenta (Syngenta Crop Protection), respectively. All larvae were reared on the roots of germinating maize seedlings until use. For both *Diabrotica* spp., third instar larvae were used for all experiments. The performance of *D. virgifera* and *D. balteata* larvae was evaluated by placing one preweighed larva into individual solo cups (Bioserv) containing moist filter paper and a 60-mg crown root section from the B73 inbred. Crown roots were covered with 50  $\mu$ L of  $\beta$ -costic acid in ethanol:water (15%:85%) to create a final tissue concentration of 100  $\mu$ g g<sup>-1</sup> fresh weight. Control roots were treated similarly with 50  $\mu$ L of ethanol:water (15%:85%). Larval growth was determined after 48 h. The preference of the root herbivores given a choice between control and  $\beta$ -costic acid-complemented roots was evaluated in 9-cm-diameter petri dishes (Greiner Bio-One). Root tissue treatments followed from the performance experiment. One root from each treatment was placed in the petri dishes. Five larvae were introduced between the two root sections, and larvae feeding behavior was recorded at 0.5, 1, 2, 3, and 4 h after the start of the trials.

## RNA Isolation and qRT-PCR

Total RNA was isolated with TRIzol (Invitrogen) according to the manufacturer's protocol. First-strand cDNA was synthesized with the RETROscript reverse transcriptase kit (Ambion) using random decamer primers. qRT-PCR was performed using Power SYBR Green Master Mix (Applied Biosystems) and 250 nm primers on a Bio-Rad CFX96 Real-Time PCR Detection System. Mean cycle threshold values of triplicate reactions were normalized to EF-1 $\alpha$  (GenBank accession no. AF136829; Huffaker et al., 2011). Fold change calculations were performed using the equation 2<sup>- $\Delta\Delta$ Ct</sup> (Livak and Schmittgen, 2001). qRT-PCR primers used in this study are listed in Supplemental Table S1.

## Isolation of *ZmTps21* cDNA from Mo17

Total RNA was isolated as described above and subjected to TURBO DNA-free treatment (Ambion) followed by total RNA purification with the RNeasy Mini protocol for RNA cleanup (Qiagen). Approximately 1  $\mu$ g of an equally mixed RNA pool from Mo17 meristem tissues elicited with heat-killed *Fusarium* spp. hyphae collected at different time points (8, 24, 32, and 48 h) was used for the construction of a 5' or 3' RACE cDNA library with the SMARTer RACE 5' / 3' Kit (Clontech) in accordance with the manufacturer's protocol. The 5' end of B73-*ZmTps21* was used to design primers for PCR amplification of the Mo17 *ZmTps21* genomic DNA. A DNA fragment, which was larger than the one from B73 on the agarose gel, was amplified using primers 5'-TGGAACCAA-CAAAGCAAGGC-3' and 5'-GAGCTCACCAATCATAGCCTC-3', cloned, and sequenced. Based on the conserved sequences between B73 and Mo17, primers were designed to amplify the 3' and 5' ends via RACE (Clontech) from 5' / 3' cDNA libraries of *Fusarium* spp. elicited meristems of Mo17. The complete cDNA sequence of the Mo17 functional *ZmTps21* was amplified with the primers Mo17 *ZmTps21*F (5'-ATGATGGTGATATTGCTGCCG-3') and Mo17 *ZmTps21*R (5'-TCAGGCACACGGCTTGAGG-3') from the Mo17 5' RACE cDNA library. Primers used to amplify *ZmTps21* genomic DNA from B73, W22, and CML247 and other diverse inbred lines (Ki3, M37W, MS71, M162W, Ki11, Mo18W, HP301, TX303, OH43, Oh7B, KY21, and Mo17) are listed in Supplemental Table S1.

## Assay for Terpene Synthase Activity

The complete open reading frame of Mo17 *ZmTps21* was amplified with the primers Mo17 *ZmTps21*-fwd (5'-CACCATGGATGGTGATATTGCTGCCG-3') and Mo17 *ZmTps21*-rev (5'-TCAGGCACACGGCTTGAGGAAC-3'), and the resulting PCR fragment was cloned into the vector pET100/D-TOPO (Invitrogen). Sequencing of several clones revealed intact Mo17 *ZmTps21* and two cloning artifacts with altered 3' ends. For heterologous expression in *Escherichia coli*, the plasmids were introduced into the strain BL21 Codon Plus (Invitrogen). Expression was induced by the addition of isopropyl-1-thio-D-galactopyranoside

to a final concentration of 1 mM. The cells were collected by centrifugation at 4,000g for 6 min and disrupted by a 4 × 30-s treatment with a sonicator in chilled extraction buffer (50 mM MOPS, pH 7, with 5 mM MgCl<sub>2</sub>, 5 mM sodium ascorbate, 0.5 mM phenylmethylsulfonyl fluoride, 5 mM DTT, and 10% [v/v] glycerol). The cell fragments were removed by centrifugation at 14,000g, and the supernatant was desalted into assay buffer (10 mM MOPS, pH 7, 1 mM DTT, and 10% [v/v] glycerol) by passage through an Econopac 10DG column (Bio-Rad). Enzyme assays were performed in a Teflon-sealed, screw-capped 1-mL GC glass vial containing 50 μL of the bacterial extract and 50 μL of assay buffer with 10 μM (*E,E*)-FPP and 10 mM MgCl<sub>2</sub>. SPME fiber sample enrichment of adsorbed reaction products and analyses by GC-MS are detailed above in "Identification and Quantification of Metabolites."

### Bioassays of in Vitro and in Vivo β-Costic Acid Activity as an Antifungal Agent

Maize antifungal assays using purified β-costic acid (Ark Pharm; no. AK168379) were performed using the Clinical and Laboratory Standards Institute M38-A2 guidelines as detailed previously (Schmelz et al., 2011). In brief, a 96-well microtiter plate-based method using a Synergy4 (BioTech Instruments) reader was used to monitor fungal growth at 30°C in broth medium through periodic measurements of changes in OD at 600 nm. Each well contained 200 μL of initial fungal inoculum (2.5 × 10<sup>4</sup> conidia mL<sup>-1</sup>) with 0.5 μL of either pure dimethyl sulfoxide or dimethyl sulfoxide containing dilutions of β-costic acid.

For the mature root infection assays with *Fusarium* spp. pathogens, individual maize plants were greenhouse grown in separate 10-L pots and supplemented with 14-14-14 Osmocote (Scotts Miracle-Gro) fertilizer. In an effort to closely parallel our observations from mature field roots and minimize the invasiveness of belowground treatments, we limited our selection to large nodal roots (2 mm or greater diameter) containing first-order lateral roots that were visually apparent and easily accessed following the temporary removal of the pot. Spanning a length of 8 cm, selected nodal roots were punctured at 1-cm intervals with a blunt-ended circular steel pin (0.6 mm diameter), creating a total of nine punctures. Divided across the nine wound sites per nodal root and depending on treatment, 100 μL of either water or 1 × 10<sup>7</sup> conidia mL<sup>-1</sup> either *Fusarium verticillioides* or *Fusarium graminearum* was applied. Treatments were limited to exposed roots growing along the outer edge of the soil in close contact with the vertical wall of the plastic pot. Following treatments, plants were carefully placed back into the pots for 7 d. For each line grown, namely B73, m050, Mo17, and m065, three treatments and four replicates were performed (4 × 4 × 3 = 48 plants). For determination of the fungal biomass, inoculated and damaged roots were collected 7 d after fungal inoculation. Total genomic DNA was extracted from the infected roots and subjected to real-time quantitative PCR using the *F. graminearum*-specific primers for a deoxynivalenol mycotoxin biosynthetic gene (*FgTri6*) and *F. verticillioides*-specific primers for a calmodulin (*FvVER1*) gene (Mule et al., 2004; Horevaj et al., 2011; Supplemental Table S1). The amount of pathogen DNA relative to plant DNA was estimated by qRT-PCR. Plant DNA quantification utilized a conserved genomic sequence of *ZmTps21/Zmtps21* DNA shared between B73 and Mo17 using forward (gTps21-F, 5'-GCAGATGTGTCGACAAGTTCC-3') and reverse (gTps21-R, 5'-TTACCTGCAGATTTCCTAAGCTCTC-3') primers with calculated amplification efficiencies of 102.65% to 102.89% between inbreds (Supplemental Table S1).

Relative amounts of fungal DNA were calculated by the 2<sup>-ΔΔCt</sup> method, normalized to a conserved genomic sequence of *ZmTps21/Zmtps21* DNA shared between B73 and Mo17.

### Statistical Analyses

ANOVA was performed on the quantified levels of terpenoids, qRT-PCR transcripts, fungal growth, and levels of fungal DNA. Treatment effects were investigated when the main effects of the ANOVA were significant (*P* < 0.05). Tukey's tests were used to correct for multiple comparisons between control and treatment groups. The short-term preference and 2-d performance of *Diabrotica* spp. larvae on roots, with and without additional β-costic acid, was analyzed with one-sample Student's *t* tests and two-way ANOVA using SigmaPlot 13.0 (Systat Software), respectively.

### Accession Numbers

Sequence data from this article can be found in the GenBank/EMBL data libraries under accession numbers MF614104, MF614105, MF614106, MF614107,

MF614108, MF614109, MF614110, MF614111, MF614112, MF614113, MF614114, and MF614115 for the inbreds Ki3, M37W, MS71, M162W, Ki11, Mo18W, HP301, TX303, OH43, Oh7B, KY21, and Mo17 respectively.

### Supplemental Data

The following supplemental materials are available.

**Supplemental Figure S1.** α/β-Selinene-derived oxidative products, β-costol, β-costal, α-costic acid, and β-costic acid, coexist as a network of maize metabolites.

**Supplemental Figure S2.** Replicated and comparative association analyses confirm the detection of *ZmTps21* as a gene candidate involved in β-costic acid biosynthesis.

**Supplemental Figure S3.** Confirmation of the locus identified by combined linkage and association mapping based on β-costic acid levels using B73 and Mo17 NILs.

**Supplemental Figure S4.** Sequence comparison of Mo17 *ZmTps21* with other plant terpene synthases known to catalyze the protonation of neutral reaction intermediates.

**Supplemental Figure S5.** *ZmTps21* gene structure and sequence polymorphisms across numerous diverse inbred lines support the occurrence of a common and conserved B73-like mutation.

**Supplemental Figure S6.** Deduced amino acid sequence comparison of *ZmTps21* across select maize inbred lines.

**Supplemental Figure S7.** C-terminal modifications in Mo17 *ZmTps21* support an influential role in the protonation of germacrene A as a putative reaction intermediate.

**Supplemental Figure S8.** Germacrene A is a minor yet detectable product of Mo17 *ZmTps21* and is converted to β-elemene during GC injection at 240°C.

**Supplemental Figure S9.** *ZmTps21*-derived products inhibit fungal growth at physiologically relevant concentrations in vitro and can be assessed in vivo using IBM NILs.

**Supplemental Table S1.** Primers used for qRT-PCR analysis and sequencing of *ZmTps21* genomic DNA.

**Supplemental Table S2.** Maize lines specifically used to identify *ZmTps21*.

### ACKNOWLEDGMENTS

We thank Dr. Adam Steinbrenner, Dr. Keini Dressano, Josh Chan, Elly Poretzky, Andrew Sher, Kinsey O'Leary, Monika Broemmer, Harley Riggelman, Susana Reyes, and Sofia Delgado for help in planting, treatments and sampling (UCSD). Natascha Rauch (Max Planck Institute for Chemical Ecology), Thibault Vassor (University of Bern) and Matisse Petit-Prost (University of Bern) are thanked for expert technical support. Dr. Laurie Smith (UCSD) is thanked for shared UCSD Biology Field Station management.

Received July 6, 2017; accepted September 18, 2017; published September 20, 2017.

### LITERATURE CITED

- Abendroth LJ, Elmore RW, Boyer MJ, Marley SK** (2011) Corn Growth and Development. Iowa State University Extension, Ames
- Ahmad S, Veyrat N, Gordon-Weeks R, Zhang Y, Martin J, Smart L, Glauser G, Erb M, Flors V, Frey M, et al** (2011) Benzoxazinoid metabolites regulate innate immunity against aphids and fungi in maize. *Plant Physiol* 157: 317–327
- Ahuja I, Kissen R, Bones AM** (2012) Phytoalexins in defense against pathogens. *Trends Plant Sci* 17: 73–90
- Ali JG, Alborn HT, Stelinski LL** (2011) Constitutive and induced subterranean plant volatiles attract both entomopathogenic and plant parasitic nematodes. *J Ecol* 99: 26–35
- Baldwin IT** (2012) Training a new generation of biologists: the genome-enabled field biologists. *Proc Am Philos Soc* 156: 205–214

- Balmer D, de Papajewski DV, Planchamp C, Glauser G, Mauch-Mani B (2013) Induced resistance in maize is based on organ-specific defence responses. *Plant J* 74: 213–225
- Baumgarten AM, Suresh J, May G, Phillips RL (2007) Mapping QTLs contributing to *Ustilago maydis* resistance in specific plant tissues of maize. *Theor Appl Genet* 114: 1229–1238
- Beck SD, Kaske ET, Smisman EE (1957) Resistance factor determination: quantitative estimation of the resistance factor, 6-methoxybenzoxazolinone, in corn plant tissue. *J Agric Food Chem* 5: 933–935
- Becker EM, Herrfurth C, Irmisch S, Köllner TG, Feussner I, Karlovsky P, Splivallo R (2014) Infection of corn ears by *Fusarium* spp. induces the emission of volatile sesquiterpenes. *J Agric Food Chem* 62: 5226–5236
- Belingeri L, Cartayrade A, Pauly G, Gleizes M (1992) Partial-purification and properties of the sesquiterpene beta-selinene cyclase from *Citrofortunella-mitis* fruits. *Plant Sci* 84: 129–136
- Berger DK, Carstens M, Korsman JN, Middleton F, Kloppers FJ, Tongoono P, Myburg AA (2014) Mapping QTL conferring resistance in maize to gray leaf spot disease caused by *Cercospora zeina*. *BMC Genet* 15: 60
- Borrego EJ, Kolomiets MV (2016) Synthesis and functions of jasmonates in maize. *Plants* (Basel) 5: 41
- Bradbury PJ, Zhang Z, Kroon DE, Casstevens TM, Ramdoss Y, Buckler ES (2007) TASSEL: software for association mapping of complex traits in diverse samples. *Bioinformatics* 23: 2633–2635
- Cane DE (1990) Enzymatic formation of sesquiterpenes. *Chem Rev* 90: 1089–1103
- Casas MI, Falcone-Ferreira ML, Jiang N, Mejía-Guerra MK, Rodríguez E, Wilson T, Engelmeier J, Casati P, Grotewold E (2016) Identification and characterization of maize salmon silks genes involved in insecticidal maysin biosynthesis. *Plant Cell* 28: 1297–1309
- Chen F, Tholl D, Bohlmann J, Pichersky E (2011) The family of terpene synthases in plants: a mid-size family of genes for specialized metabolism that is highly diversified throughout the kingdom. *Plant J* 66: 212–229
- Christensen SA, Huffaker A, Kaplan F, Sims J, Ziemann S, Doehlemann G, Ji L, Schmitz RJ, Kolomiets MV, Alborn HT, et al (2015) Maize death acids, 9-lipoxygenase-derived cyclopentane(a)nonenes, display activity as cytotoxic phytoalexins and transcriptional mediators. *Proc Natl Acad Sci USA* 112: 11407–11412
- Churchill GA, Doerge RW (1994) Empirical threshold values for quantitative trait mapping. *Genetics* 138: 963–971
- Cook JP, McMullen MD, Holland JB, Tian F, Bradbury P, Ross-Ibarra J, Buckler ES, Flint-Garcia SA (2012) Genetic architecture of maize kernel composition in the nested association mapping and inbred association panels. *Plant Physiol* 158: 824–834
- Couture RM, Routley DG, Dunn GM (1971) Role of cyclic hydroxamic acids in monogenic resistance of maize to *Helminthosporium turcicum*. *Physiol Plant Pathol* 1: 515–521
- Dangl JL, Horvath DM, Staskawicz BJ (2013) Pivoting the plant immune system from dissection to deployment. *Science* 341: 746–751
- Degenhardt J (2009) Indirect defense responses to herbivory in grasses. *Plant Physiol* 149: 96–102
- Degenhardt J, Hiltbold I, Köllner TG, Frey M, Gierl A, Gershenzon J, Hibbard BE, Ellersieck MR, Turlings TCJ (2009a) Restoring a maize root signal that attracts insect-killing nematodes to control a major pest. *Proc Natl Acad Sci USA* 106: 13213–13218
- Degenhardt J, Köllner TG, Gershenzon J (2009b) Monoterpene and sesquiterpene synthases and the origin of terpene skeletal diversity in plants. *Phytochemistry* 70: 1621–1637
- de Kraker JW, Franssen MCR, de Groot A, Shibata T, Bouwmeester HJ (2001) Germacrenes from fresh costus roots. *Phytochemistry* 58: 481–487
- Eichten SR, Foerster JM, de Leon N, Kai Y, Yeh CT, Liu S, Jeddeloh JA, Schnable PS, Kaeppler SM, Springer NM (2011) B73-Mo17 near-isogenic lines demonstrate dispersed structural variation in maize. *Plant Physiol* 156: 1679–1690
- Elshire RJ, Glaubitz JC, Sun Q, Poland JA, Kawamoto K, Buckler ES, Mitchell SE (2011) A robust, simple genotyping-by-sequencing (GBS) approach for high diversity species. *PLoS ONE* 6: e19379
- Flint-Garcia SA, Dashiell KE, Prischmann DA, Bohn MO, Hibbard BE (2009) Conventional screening overlooks resistance sources: rootworm damage of diverse inbred lines and their B73 hybrids is unrelated. *J Econ Entomol* 102: 1317–1324
- Flint-Garcia SA, Thuillet AC, Yu J, Pressoir G, Romero SM, Mitchell SE, Doebley J, Kresovich S, Goodman MM, Buckler ES (2005) Maize association population: a high-resolution platform for quantitative trait locus dissection. *Plant J* 44: 1054–1064
- Frey M, Schullehner K, Dick R, Fiesselmann A, Gierl A (2009) Benzoxazinoid biosynthesis, a model for evolution of secondary metabolic pathways in plants. *Phytochemistry* 70: 1645–1651
- Fu J, Ren F, Lu X, Mao H, Xu M, Degenhardt J, Peters RJ, Wang Q (2016) A tandem array of ent-kaurene synthases in maize with roles in gibberellin and more specialized metabolism. *Plant Physiol* 170: 742–751
- Gardiner JM, Coe EH, Melia-Hancock S, Hoisington DA, Chao S (1993) Development of a core RFLP map in maize using an immortalized F2 population. *Genetics* 134: 917–930
- Gassmann AJ, Petzold-Maxwell JL, Keweshan RS, Dunbar MW (2011) Field-evolved resistance to Bt maize by western corn rootworm. *PLoS ONE* 6: e22629
- Gershenzon J, Dudareva N (2007) The function of terpene natural products in the natural world. *Nat Chem Biol* 3: 408–414
- Gershenzon J, Kreis W (1999) Biosynthesis of Monoterpenes, Sesquiterpenes, Diterpenes, Sterols, Cardiac Glycosides and Steroid Saponins. Sheffield Academic Press, Sheffield, UK
- Gray ME, Sappington TW, Miller NJ, Moeser J, Bohn MO (2009) Adaptation and invasiveness of western corn rootworm: intensifying research on a worsening pest. *Annu Rev Entomol* 54: 303–321
- Handrick V, Robert CAM, Ahern KR, Zhou S, Machado RAR, Maag D, Glauser G, Fernandez-Penny FE, Chandran JN, Rodgers-Melnik E, et al (2016) Biosynthesis of 8-O-methylated benzoxazinoid defense compounds in maize. *Plant Cell* 28: 1682–1700
- Harborne JB (1999) The comparative biochemistry of phytoalexin induction in plants. *Biochem Syst Ecol* 27: 335–367
- Hirsch CN, Foerster JM, Johnson JM, Sekhon RS, Muttoni G, Vaillancourt B, Peñagaricano F, Lindquist E, Pedraza MA, Barry K, et al (2014) Insights into the maize pan-genome and pan-transcriptome. *Plant Cell* 26: 121–135
- Horevaj P, Milus EA, Bluhm BH (2011) A real-time qPCR assay to quantify *Fusarium graminearum* biomass in wheat kernels. *J Appl Microbiol* 111: 396–406
- Huffaker A, Kaplan F, Vaughan MM, Dafoe NJ, Ni X, Rocca JR, Alborn HT, Teal PEA, Schmelz EA (2011) Novel acidic sesquiterpenoids constitute a dominant class of pathogen-induced phytoalexins in maize. *Plant Physiol* 156: 2082–2097
- Huffaker A, Pearce G, Veyrat N, Erb M, Turlings TCJ, Sartor R, Shen Z, Briggs SP, Vaughan MM, Alborn HT, et al (2013) Plant elicitor peptides are conserved signals regulating direct and indirect antiherbivore defense. *Proc Natl Acad Sci USA* 110: 5707–5712
- Iijima Y, Davidovich-Rikanati R, Fridman E, Gang DR, Bar E, Lewinsohn E, Pichersky E (2004) The biochemical and molecular basis for the divergent patterns in the biosynthesis of terpenes and phenylpropenes in the peltate glands of three cultivars of basil. *Plant Physiol* 136: 3724–3736
- Katerinopoulos EH, Isaakidis D, Sofou K, Spyros A (2011) Use of costic acid or extracts of *Dittrichia viscosa* against *Varroa destructor*. Google Patents WO2009153607 A1, December 23, 2009
- Köllner TG, Held M, Lenk C, Hiltbold I, Turlings TCJ, Gershenzon J, Degenhardt J (2008a) A maize (*E*)- $\beta$ -caryophyllene synthase implicated in indirect defense responses against herbivores is not expressed in most American maize varieties. *Plant Cell* 20: 482–494
- Köllner TG, Lenk C, Schnee C, Köpke S, Lindemann P, Gershenzon J, Degenhardt J (2013) Localization of sesquiterpene formation and emission in maize leaves after herbivore damage. *BMC Plant Biol* 13: 15
- Köllner TG, Schnee C, Gershenzon J, Degenhardt J (2004a) The sesquiterpene hydrocarbons of maize (*Zea mays*) form five groups with distinct developmental and organ-specific distributions. *Phytochemistry* 65: 1895–1902
- Köllner TG, Schnee C, Gershenzon J, Degenhardt J (2004b) The variability of sesquiterpenes emitted from two *Zea mays* cultivars is controlled by allelic variation of two terpene synthase genes encoding stereoselective multiple product enzymes. *Plant Cell* 16: 1115–1131
- Köllner TG, Schnee C, Li S, Svatos A, Schneider B, Gershenzon J, Degenhardt J (2008b) Protonation of a neutral (*S*)- $\beta$ -bisabolene intermediate is involved in (*S*)- $\beta$ -macrocyclic formation by the maize sesquiterpene synthases TPS6 and TPS11. *J Biol Chem* 283: 20779–20788
- Lanubile A, Ferrarini A, Maschietto V, Delledonne M, Marocco A, Bellin D (2014) Functional genomic analysis of constitutive and inducible defense responses to *Fusarium verticillioides* infection in maize genotypes with contrasting ear rot resistance. *BMC Genomics* 15: 710

- Lee M, Sharopova N, Beavis WD, Grant D, Katt M, Blair D, Hallauer A (2002) Expanding the genetic map of maize with the intermated B73 × Mo17 (IBM) population. *Plant Mol Biol* **48**: 453–461
- Lipka AE, Tian F, Wang Q, Peiffer J, Li M, Bradbury PJ, Gore MA, Buckler ES, Zhang Z (2012) GAPIT: genome association and prediction integrated tool. *Bioinformatics* **28**: 2397–2399
- Livak KJ, Schmittgen TD (2001) Analysis of relative gene expression data using real-time quantitative PCR and the 2(-Delta Delta C(T)) method. *Methods* **25**: 402–408
- McMullen MD, Frey M, Degenhardt J (2009a) Genetics and biochemistry of insect resistance in maize. In: JL Bennetzen, SC Hake, eds, *Handbook of Maize: Its Biology*. Springer, New York, pp 271–289
- McMullen MD, Kresovich S, Villeda HS, Bradbury P, Li H, Sun Q, Flint-Garcia S, Thornsberry J, Acharya C, Bottoms C, et al (2009b) Genetic properties of the maize nested association mapping population. *Science* **325**: 737–740
- Meihls LN, Handrick V, Glauser G, Barbier H, Kaur H, Haribal MM, Lipka AE, Gershenzon J, Buckler ES, Erb M, et al (2013) Natural variation in maize aphid resistance is associated with 2,4-dihydroxy-7-methoxy-1,4-benzoxazin-3-one glucoside methyltransferase activity. *Plant Cell* **25**: 2341–2355
- Meinke LJ, Sappington TW, Onstad DW, Guillemaud T, Miller NJ, Judith K, Nora L, Furlan L, Jozsef K, Ferenc T (2009) Western corn rootworm (*Diabrotica virgifera virgifera* LeConte) population dynamics. *Agric For Entomol* **11**: 29–46
- Meyer JDF, Snook ME, Houchins KE, Rector BG, Widstrom NW, McMullen MD (2007) Quantitative trait loci for maysin synthesis in maize (*Zea mays* L.) lines selected for high silk maysin content. *Theor Appl Genet* **115**: 119–128
- Miller NJ, Guillemaud T, Giordano R, Siegfried BD, Gray ME, Meinke LJ, Sappington TW (2009) Genes, gene flow and adaptation of *Diabrotica virgifera virgifera*. *Agric For Entomol* **11**: 47–60
- Mule G, Susca A, Stea G, Moretti A (2004) A species-specific PCR assay based on the calmodulin partial gene for identification of *Fusarium verticillioides*, *F. proliferatum* and *F. subglutinans*. *Eur J Plant Pathol* **110**: 495–502
- Nguyen DT, Göpfert JC, Ikezawa N, Macnevin G, Kathiresan M, Conrad J, Spring O, Ro DK (2010) Biochemical conservation and evolution of germacrene A oxidase in Asteraceae. *J Biol Chem* **285**: 16588–16598
- Olukolu BA, Tracy WF, Wisser R, De Vries B, Balint-Kurti PJ (2016) A genome-wide association study for partial resistance to maize common rust. *Phytopathology* **106**: 745–751
- Rao KV, Alvarez FM (1981) Antibiotic principle of *Eupatorium capillifolium*. *J Nat Prod* **44**: 252–256
- Rasmann S, Köllner TG, Degenhardt J, Hiltpold I, Toepfer S, Kuhlmann U, Gershenzon J, Turlings TCJ (2005) Recruitment of entomopathogenic nematodes by insect-damaged maize roots. *Nature* **434**: 732–737
- Richter A, Schaff C, Zhang Z, Lipka AE, Tian F, Köllner TG, Schnee C, Preiß S, Irmisch S, Jander G, et al (2016) Characterization of biosynthetic pathways for the production of the volatile homoterpenes DMNT and TMTT in *Zea mays*. *Plant Cell* **28**: 2651–2665
- Saba F (1970) Host plant spectrum and temperature limitations of *Diabrotica balteata*. *Can Entomol* **102**: 684
- Samayoa LF, Malvar RA, Olukolu BA, Holland JB, Butrón A (2015) Genome-wide association study reveals a set of genes associated with resistance to the Mediterranean corn borer (*Sesamia nonagrioides* L.) in a maize diversity panel. *BMC Plant Biol* **15**: 35
- Schmelz EA, Alborn HT, Tumlinson JH (2001) The influence of intact-plant and excised-leaf bioassay designs on volicitin- and jasmonic acid-induced sesquiterpene volatile release in *Zea mays*. *Planta* **214**: 171–179
- Schmelz EA, Engelberth J, Alborn HT, Tumlinson JH III, Teal PEA (2009) Phytohormone-based activity mapping of insect herbivore-produced elicitors. *Proc Natl Acad Sci USA* **106**: 653–657
- Schmelz EA, Engelberth J, Tumlinson JH, Block A, Alborn HT (2004) The use of vapor phase extraction in metabolic profiling of phytohormones and other metabolites. *Plant J* **39**: 790–808
- Schmelz EA, Huffaker A, Sims JW, Christensen SA, Lu X, Okada K, Peters RJ (2014) Biosynthesis, elicitation and roles of monocot terpenoid phytoalexins. *Plant J* **79**: 659–678
- Schmelz EA, Kaplan F, Huffaker A, Dafoe NJ, Vaughan MM, Ni X, Rocca JR, Alborn HT, Teal PE (2011) Identity, regulation, and activity of inducible diterpenoid phytoalexins in maize. *Proc Natl Acad Sci USA* **108**: 5455–5460
- Schnable PS, Ware D, Fulton RS, Stein JC, Wei F, Pasternak S, Liang C, Zhang J, Fulton L, Graves TA, et al (2009) The B73 maize genome: complexity, diversity, and dynamics. *Science* **326**: 1112–1115
- Schnee C, Köllner TG, Gershenzon J, Degenhardt J (2002) The maize gene terpene synthase 1 encodes a sesquiterpene synthase catalyzing the formation of (*E*)- $\beta$ -farnesene, (*E*)-nerolidol, and (*E,E*)-farnesol after herbivore damage. *Plant Physiol* **130**: 2049–2060
- Schnee C, Köllner TG, Held M, Turlings TCJ, Gershenzon J, Degenhardt J (2006) The products of a single maize sesquiterpene synthase form a volatile defense signal that attracts natural enemies of maize herbivores. *Proc Natl Acad Sci USA* **103**: 1129–1134
- Sowbhagya HB (2014) Chemistry, technology, and nutraceutical functions of celery (*Apium graveolens* L.): an overview. *Crit Rev Food Sci Nutr* **54**: 389–398
- Spencer JL, Hibbard BE, Moeser J, Onstad DW (2009) Behaviour and ecology of the western corn rootworm (*Diabrotica virgifera virgifera* LeConte). *Agric For Entomol* **11**: 9–27
- Starks CM, Back K, Chappell J, Noel JP (1997) Structural basis for cyclic terpene biosynthesis by tobacco 5-*epi*-aristolochene synthase. *Science* **277**: 1815–1820
- Tinsley NA, Estes RE, Gray ME (2013) Validation of a nested error component model to estimate damage caused by corn rootworm larvae. *J Appl Entomol* **137**: 161–169
- Turlings TCJ, Tumlinson JH, Lewis WJ (1990) Exploitation of herbivore-induced plant odors by host-seeking parasitic wasps. *Science* **250**: 1251–1253
- Turner SD (2014) qqman: an R package for visualizing GWAS results using QQ and Manhattan plots. *bioRxiv* <http://dx.doi.org/10.1101/005165>
- VanEttten HD, Mansfield JW, Bailey JA, Farmer EE (1994) Two classes of plant antibiotics: phytoalexins versus “phytoanticipins.” *Plant Cell* **6**: 1191–1192
- VanRaden PM (2008) Efficient methods to compute genomic predictions. *J Dairy Sci* **91**: 4414–4423
- Vaughan MM, Christensen S, Schmelz EA, Huffaker A, McAuslane HJ, Alborn HT, Romero M, Allen LH, Teal PEA (2015) Accumulation of terpenoid phytoalexins in maize roots is associated with drought tolerance. *Plant Cell Environ* **38**: 2195–2207
- Wu QX, Shi YP, Jia ZJ (2006) Eudesmane sesquiterpenoids from the Asteraceae family. *Nat Prod Rep* **23**: 699–734
- Yan J, Lipka AE, Schmelz EA, Buckler ES, Jander G (2015) Accumulation of 5-hydroxynorvaline in maize (*Zea mays*) leaves is induced by insect feeding and abiotic stress. *J Exp Bot* **66**: 593–602
- Yu J, Pressoir G, Briggs WH, Vroh Bi I, Yamasaki M, Doebley JF, McMullen MD, Gaut BS, Nielsen DM, Holland JB, et al (2006) A unified mixed-model method for association mapping that accounts for multiple levels of relatedness. *Nat Genet* **38**: 203–208
- Zhang Z, Ersoz E, Lai CQ, Todhunter RJ, Tiwari HK, Gore MA, Bradbury PJ, Yu J, Arnett DK, Ordovas JM, et al (2010) Mixed linear model approach adapted for genome-wide association studies. *Nat Genet* **42**: 355–360